Determining properties of evolved hot stars with winds from UV observations

Graziela R. Keller[1], Luciana Bianchi[2], James E. Herald, Walter J. Maciel[1]

[1]Universidade de São Paulo/USP -Brazil [2]The Johns Hopkins University - USA

Abstract

Central stars of planetary nebulae (CSPNe) are characterized by very high temperatures and surface gravities and may present strong wind features, most conspicuous on the UV. Solid determinations of their stellar parameters are necessary to tackle questions concerning stellar evolution and possible evolutionary links among different CSPN sub-types, the wind driving mechanism and the properties of the surrounding nebulae. UV and Far-UV observations are important for measuring the terminal velocity of the wind and constraining wind clumping to measure accurate mass loss rates. These spectral regions also show important diagnostic lines of highly ionized iron, argon and neon and, in the case of very hot [WCE] CSPNe, the few available lines of multiple ionization stages of a given element. We derived wind and photospheric parameters for a H-deficient CSPNe sample from HST/STIS, FUSE and IUE UV and Far-UV observations. We also present grids of synthetic spectra (Keller et al. 2011), calculated using the CMFGEN non-LTE stellar atmosphere code (Hillier & Miller 1998), which accounts for spherically symmetric stationary expanding atmospheres, line blanketing and wind clumping. The grids include many ionic species previously neglected, facilitate line identification and are an important tool to plan observations.

Grids of Synthetic Spectra

The stellar parameters adopted for the grid models are within typical literature values for **H-poor CSPNe** and approximately follow the evolutionary calculations of Miller Bertolami & Althaus (2006).

The ionic species included in the models can vary, since they were limited to keep the models within a workable size. All models have the following species: He I, He II, He III, C IV, C V, N V, N VI, O V, O VI, OVII, Ne V, Ne VI, Ne VII, Ne VIII, Ne IX, Si IV, Si V, P V, P VI, S VI, S VII, Fe VII, Fe VIII, Fe IX, Fe X, Fe XI. The other ionic species, which include C II, C III, N II, N III, N IV, O II, O III, O IV, Ne II, Ne III, Ne IV, Al III, Al IV, Al V, Si III, Si VI, P IV, S III, S IV, S V, Fe IV, Fe V, Fe VI, were added as needed

The grids are available at http://dolomiti.pha.jhu.edu/planetarynebulae.html.

Grid Models' Abundances

Element	Mass Fraction
He	0.43
C	0.45
N	0.01
O	0.08
Ne	0.02
Al	5.57×10^{-5}
Si	6.99×10^{-4}
P	6.12×10^{-6}
S	3.82×10^{-4}
Fe	1.36×10^{-5}

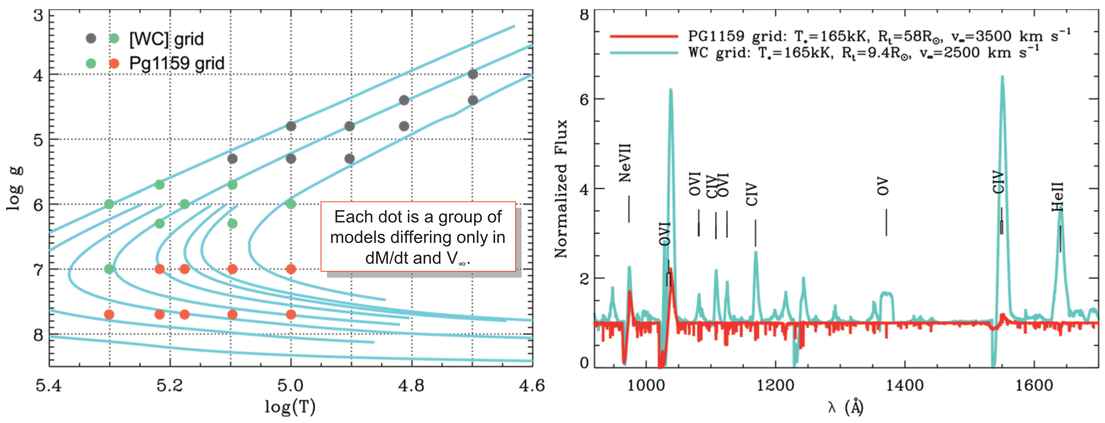

Figure 1. Left panel: the [WC] (gray and green dots) and PG1159 (green and orange dots) grids of synthetic spectra are shown on the log(T) X log(g) diagram, along with evolutionary calculations from Miller Bertolami & Althaus (2006), in blue. Right panel: comparison between similar temperature synthetic spectra from the PG1159 and the [WC] grids. The PG1159 models have fainter winds that reach higher terminal velocities than the ones from the [WC] grid models.

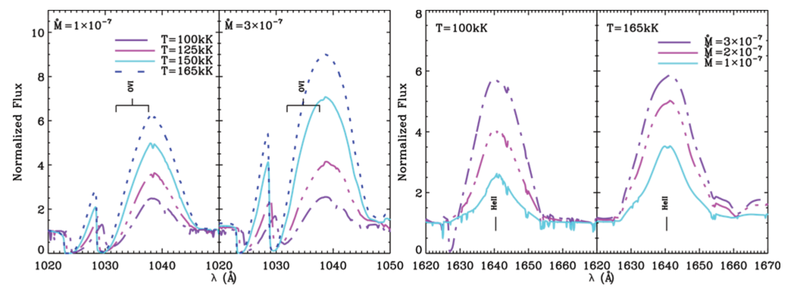

Figure 2. Synthetic line profiles from the [WC] grid models of different mass-loss rates and temperatures. The left and right panels illustrate the behavior of the far-UV O VI λλ 1031.9, 1037.6 Å doublet and the He II λ 1640.4 Å line with changing stellar parameters, respectively.

Effect of the LSF on the Synthetic Spectra

The grids can be used to plan the observations, determining the necessary instrument specifications, particularly if the shapes of the LSFs (not just their FWHM) fit the requirements of the desired measurement.

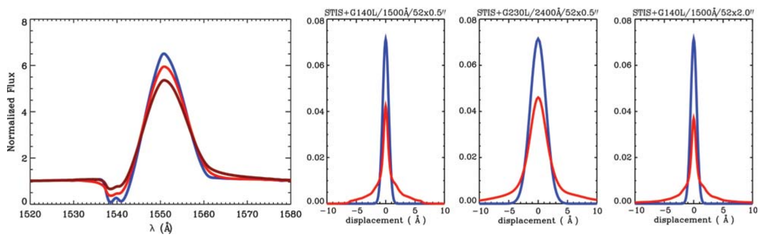

Figure 3. Left panel: C IV λλ 1548.2, 1550.8 Å synthetic line profile from a grid model convolved with: a Gaussian of FWHM equal to the nominal resolution of the G140L difraction grating from the STIS spectrograph (blue line), with the G140L instrumental LSF for the 52x0.5" apperture (red line), and for the 52x2.0" apperture (dark red line). Other panels: the HST STIS LSFs (red lines) are compared to Gaussians (blue lines) with FWHM equal to the nominal spectral resolution of the configuration.

GRK acknowledges FAPESP and CAPES grants 2012/03479-2, 06/58240-3 and 0370-09-6.

The data presented here were obtained from MAST.

References

Hillier, D.J., Miller, D.L., 1998, ApJ, 496, 407
Keller, G. R., Herald, J. E., Bianchi L., Maciel, W. J., Bohlin R. C., 2011, MNRAS, 418, 705
Miller Bertolami, M. M., Althaus, L. G., 2006. A&A, 454, p. 845

http://www.astro.iag.usp.br/~graziela

UV Spectral Analysis

Our uniform model set enables systematic analysis of observed spectra to constrain stellar parameters. We used them to analyze UV and far-UV spectra of the hot [WCE] central stars of NGC 6905, NGC 5189 and Sand 3 and constrain their main stellar parameters.

Data

Object	Instrument	Resolution [Å]	Aperture [arcsec]	Range [Å]
NGC 6905	FUSE	~0.06	30x30	905-1187
	STIS+G140L	~1.20	52x0.5	1150-1736
	STIS+G230L	~3.15	52x0.5	1570-3180
NGC 5189	FUSE	~0.06	30x30	905-1187
	IUE	~7.0	9.3x20.7	1851-3349
	IUE	~6.0	8.9x21.6	1151-1979
Sand 3	STIS+G140L	~1.20	52x2	1128-1725
	STIS+G230MB	~0.33	52x2	2198-2353
	STIS+G230MB	~0.33	52x2	2717-2871
	IUE	~6.0	8.9x21.6	1151-1979
	IUE	~7.0	9.3x20.7	1851-3349

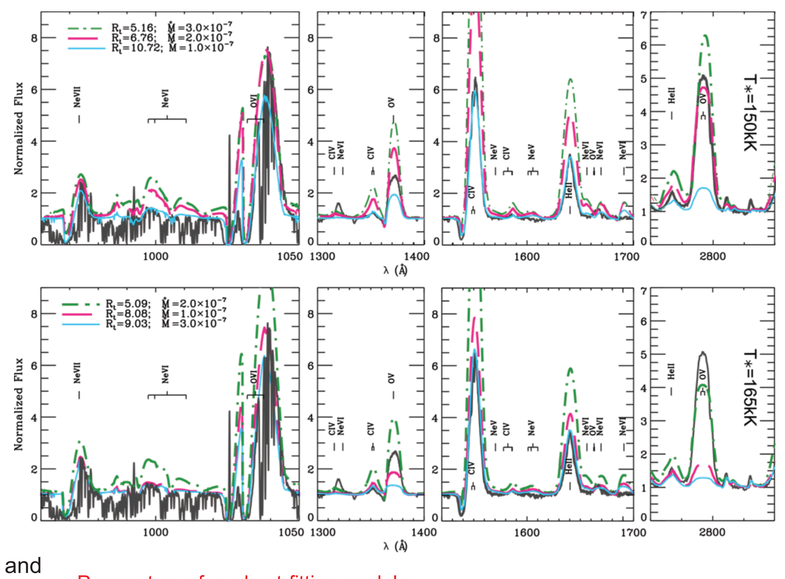

Figure 4. UV and far-UV observed spectra (continuous black line) of the central star of NGC 6905 and grid models (colored lines) with T*=150 and 165 kK and various values of transformed radius (transformed radii and mass-loss rates are given in units of $R_\odot$ and $M_\odot yr^{-1}$, respectively). All the models shown have v_∞=2000 km s^{-1}. The transformed radius, Rt, is defined as

$$R_t = R_* \left[\frac{v_\infty / 2500\ km\ s^{-1}}{\dot{M}/10^{-4}\ M_\odot yr^{-1}} \right]^{2/3}$$

Having constrained the Rt and T*, we then varied other parameters not covered by the main grids, such as elemental abundances and the inclusion of new elements into the calculations.

Parameters of our best-fitting models

Object	T*[kK]	$R_t[R_\odot]$	v_∞[km/s]	X_{He}	X_C	X_N	X_O	X_{Ne}
NGC 6905	150	10.7	2000	0.44	0.45	1.1×10^{-4}	0.08	0.02
NGC 5189	165	10.5	2500	0.58	0.25	0.01	0.12	0.04
Sand 3	150	9.3	2000	0.28	0.55	0.07	0.08	0.02

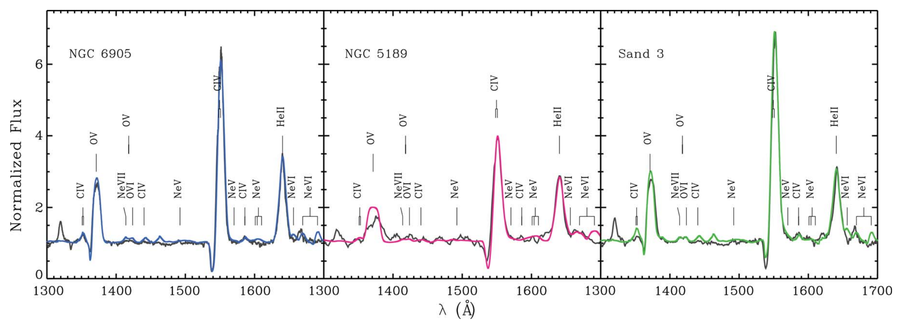

Figure 5. Right: observed spectra (black lines) of the central stars of NGC 6905, NGC 5189 and Sand 3 and our best fit models (colored lines).

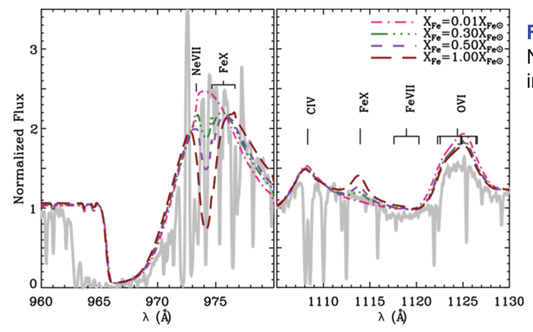

Figure 6. Left: observed spectra (light grey continuous line) of NGC 5189's central star compared with models of different iron content (dashed lines).

Figure 7. Below: in black, we show the observed spectra of the central star of NGC 6905. The light blue line is our best-fitting model. In pink, this same model is shown affected by interstellar absorption by molecular hydrogen with a column density given by $\log N(H_2)$=19.5

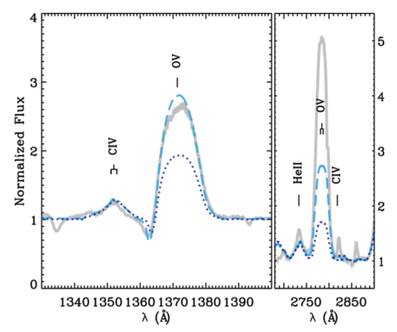

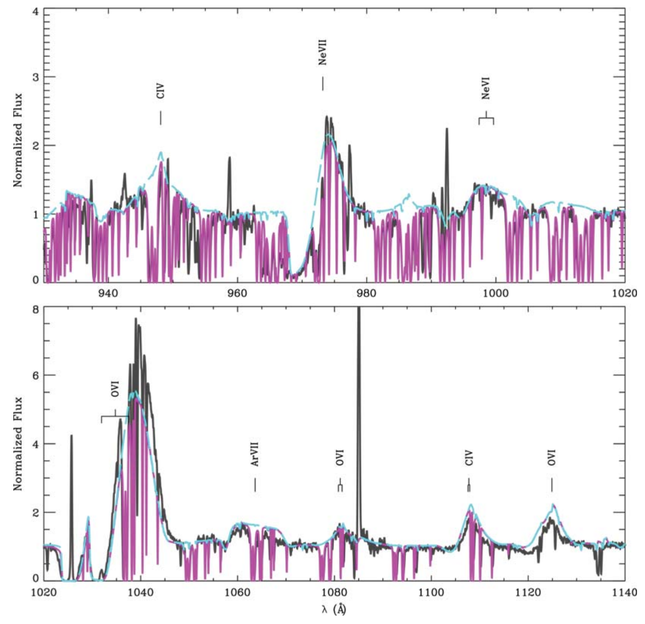

Figure 8. Above: spectra of NGC 6905's central star (light grey continuous line) compared with synthetic spectra computed with (dashed line) and without (dotted line) Mg, Na, Co, and Ni. The effect is seen on the O V lines only.